Single top production as a probe of B^{′} quarks

Joseph W. Nutter, Reinhard Schwienhorst, Devin G. E. Walker, and Jiang-Hao Yu

Phys. Rev. D **86**, 094006 — Published 1 November 2012

DOI: 10.1103/PhysRevD.86.094006

Single Top Production as a Probe of B′ Quarks

Joseph W. Nutter,[1] Reinhard Schwienhorst,[1] Devin G. E. Walker,[2] and Jiang-Hao Yu[1]

[1]*Department of Physics and Astronomy, Michigan State University, East Lansing MI 48824, USA*
[2]*SLAC National Accelerator Laboratory, 2575 Sand Hill Road, Menlo Park, CA 94025, USA*

(Dated: September 14, 2012)

We show how single top production at the LHC can be used to discover (and characterize the couplings of) B' quarks, which are an essential part of many natural models of new physics beyond the Standard Model. We present the B' effective model and concentrate on resonant production via a colored anomalous magnetic moment. Generally, B's preferentially decay into a single top quark produced in association with a W boson; thus, this production process makes associated single top production essential to B' searches at the LHC. We demonstrate the background processes are manageable and the signal cross section is sufficient to yield a large signal significance even during the 7 TeV LHC run. Specifically, we show that B' masses of 700 GeV or more can be probed. Moreover, if a B' is found, then the chirality of its coupling can be determined. Finally, we present signal cross sections for several different LHC energies.

PACS numbers: 14.65.Jk, 14.65.Ha, 12.60.-i

I. INTRODUCTION

For the first time in history, the TeV scale is being directly probed by the Large Hadron Collider (LHC). Remarkably, a 125 GeV Higgs-like particle [1, 2] has already been discovered. Beyond this tremendous achievement, an additional focus of the LHC is to uncover new particles which will presage new physics scenarios. Fourth generation B' quarks are an example of such a new particle. They are essential to many new physics scenarios and could appear as a chiral or vector-like quark. A sample of popular models with B' quarks (or the strongly coupled equivalent) can be found in [3–10]. In Section II, we further detail the role B' quarks in natural models and focus on their outsized importance in model building in avoidance of precision electroweak constraints.

Final states involving single top quarks provide an important discovery mode for B' quarks that has not been explored heretofore. Moreover, given sufficient data, the single top final state is uniquely sensitive to the chirality of the B' quark. The LHC has been remarkably adept at searching for single top events. About three million single top events should have been recorded (after cuts) during the 7 TeV LHC run [11, 12]. Additionally, evidence for SM $W\,t$ production was presented [13]. More importantly, the production cross section for SM single top events is precisely known at NLO with NNLO corrections [14]. We present an effective model for B' quark production and decay during the LHC runs at 7 TeV, 8 TeV and 14 TeV center-of-mass (c.m.) energies. We explore the signal and backgrounds for a $B' \to W\,t$ single top search in the lepton+jets final state. This work should be considered as complementary to B' pair production which subsequently decays to top quark pairs. The combination of the two signatures should be part of a comprehensive plan to maximizes the sensitivity of the LHC to natural new physics. To date, the B' searches from the Tevatron and the LHC have relied exclusively on the pair-production mode, in searches for SM-like decays of the fourth generation quark [15–17] and in searches for chiral and vector-like B' quarks [18–20].

This paper is organized in the following way: In Section II, we describe the constraints and implication of B' models on new physics beyond the Standard Model. Next in Section III, we outline our effective B' models and conventions. We detail a benchmark scenario which is simulated and analyzed in the subsequent sections. Section IV gives the cross section for the $p\,p \to B' \to W\,t$ process. The phenomenological analysis is described in Section V, including the various backgrounds expected at the LHC. Finally we conclude.

II. B' MODELS, NATURALNESS AND PRECISION MEASUREMENTS

A. Naturalness and New Physics Scales

It is well known that a light 125 GeV Higgs boson [1, 2] illustrates a serious theoretical inconsistency in the Standard Model. Radiative corrections, generated dominantly by top quark loops, push the Higgs boson to have a mass of order the next largest scale of new physics. Thus, since the Planck scale is only known scale beyond the weak scale, naively the Higgs boson should have a mass of order 10^{19} GeV. This implies the couplings in the Higgs potential must be severely fine-tuned in order to get the right electroweak symmetry breaking vev. Natural models of new physics solve this problem by adding new top partners to the SM which cancel (some or all of) the top quark radiative corrections. These top partners *must* be in an electroweak doublet in order to properly cancel the divergences to the Higgs mass by the SM top quark. Thus, many natural models also feature B' quarks, the heavy partner of the bottom quark. Consequently, discovering a B' quark may be a harbinger of new natural physics beyond the SM. Moreover, if the top and bottom partners have the same mass hierarchy as the SM top and bottom, the B' quark may be the first to be discovered.

There is more to this story of top partners, naturalness and new heavy quarks. It has been shown [21, 22] that partial wave unitarity can place an upper bound on the mass of additional heavy fermions which obtain *all* of their mass from electroweak symmetry breaking. For heavy B' quarks, this limit is

$$m_{B'} < 500/\sqrt{N}\ \text{GeV} \tag{1}$$

where N counts the number of degenerate $SU(2)_L$ doublets. Natural models get around this bound by requiring a new scale of physics [3–10]. We show that 500 GeV B' quark masses can easily be seen during the 7 TeV run at the LHC. A heavier B' quark would imply a new scale of physics beyond the SM. It also implies that the 7 TeV LHC run can rule out traditional fourth generation B's which get all of their mass from electroweak symmetry breaking.

B. Bounds on B' Models from Precision Measurements

Models with exact custodial symmetry generate minimal corrections to the well-constrained S and T parameters [23]. Custodial symmetries are therefore a common feature of natural new physics beyond the Standard Model. Because of this, and the fact that natural models feature a large coupling between the top partner and the SM, implicitly the bottom partner also has a significant coupling [37]. After spontaneous symmetry breaking, the top and bottom partners can mix with the SM third generation. This mixing can potentially lead to large corrections to $Z \to \overline{b}\, b$. Indeed, precision measurements from LEP and SLAC require less than 0.3% deviation [24] from the SM prediction for this process. Yet new models of electroweak symmetry breaking (e.g. extra-dimensional scenarios) can generate 20-40% corrections. It was recognized that an "extended" custodial symmetry could be arranged to prevent large corrections to $Z \to \overline{b}_L b_L$ but not $Z \to \overline{t}_L\, t_L$ and $W \to \overline{t}_L\, b_L$ simultaneously [25]. This symmetry is

$$O(4) \sim SU(2)_L \times SU(2)_R \times P_{LR}, \tag{2}$$

where P_{LR} is a parity interchanging left and right. It has also been shown there can be tensions between $Z \to \overline{b}\, b$ constraints and the T parameter for another extended custodial symmetry [26]. Our single top signal directly probes the $W \to \overline{t}_L\, b_L$ coupling and the mixing between the B' and b quarks. Thus, the nature of the custodial symmetry is a consequence of the search for bottom partners. Limits from b-quark strong interactions also do not provide a constraint [27].

III. EFFECTIVE COUPLINGS AND CONVENTIONS

A. Effective Lagrangian

To probe B' models, we consider an effective scenario where a new B' quark is the only light state below a cutoff [38]. The most general Lagrangian describing the interactions of heavy bottom quarks with gluons (assuming operators of dimension five or less) is [28]

$$\mathcal{L} = g_s \, \overline{B'} \gamma^\mu G_\mu B' + \frac{g_s \, \lambda}{2 \, \Lambda} G_{\mu\nu} \, \overline{b} \, \sigma^{\mu\nu} \left(\kappa_L^b P_L + \kappa_R^b P_R \right) B' + \text{h.c.} \tag{3}$$

The dimension five operator is generated in many models [3–10] by integrating out new states. Here we follow convention and set the scale Λ to $M_{B'}$. $P_{L,R}$ are the normal projection operators, while λ is a free parameter whose value is dependent on the UV physics that was integrated out. We set $\lambda = 1$ [28]. We focus on the coupling with gluons because of the large fraction of gluon initial state partons at LHC energies. Similar operators can generate flavor-changing-neutral-currents (FCNC). We assume the UV theory is free of FCNCs, therefore ensuring that λ/Λ is sufficiently suppressed.

The electroweak decay of the B' quark into a single top quark can be parametrized as

$$\mathcal{L} = \frac{g_2}{\sqrt{2}} \, W_\mu^+ \, \overline{t} \gamma^\mu \left(f_L P_L + f_R P_R \right) B' + \text{h.c.} \tag{4}$$

Here g_2 is the $SU(2)_L$ coupling. In the case where a left-handed (chiral or vector-like) quark mixes with the left-handed bottom quark, the couplings are

$$f_L = s_L, \quad f_R \simeq 0 \, . \tag{5}$$

For the right-handed case, the couplings are

$$f_L \simeq 0, \quad f_R = s_R \, . \tag{6}$$

The partial decay width of the B' quark to Wt is given by

$$\Gamma(B \to t \, W^-) = \frac{g_2^2}{64\pi} \frac{M_B^3}{M_W^2} (f_L^2 + f_R^2)(1 - x_t^2)^3 + \mathcal{O}(x_W^2) \, . \tag{7}$$

We consider a B' benchmark scenario with couplings $s_L = s_R = \frac{v}{m_{B'}}$, $\kappa_L = \kappa_R = 0.5$. With these settings, the total decay width at a B' mass of 700 GeV is 31.85 GeV. The branching ratio, together with those for bg, bZ and bH decays are shown in Fig. 1. (See the Appendix for those partial decay widths.) At low masses, the bZ and bH decays dominate, while at higher masses the Wt decay is the largest and approaches 40% of the total width. The large decay branching ratio to Wt makes this an attractive final state for a B' search.

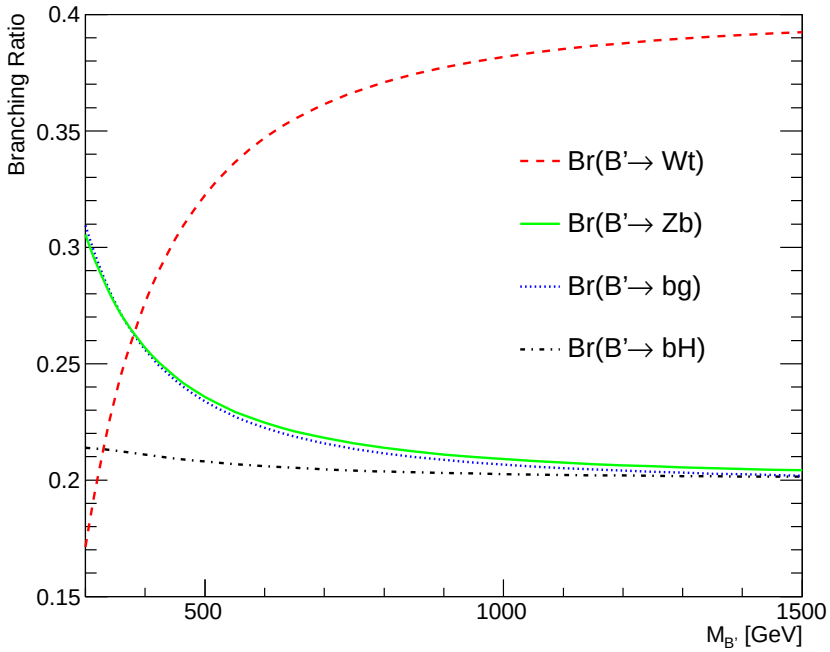

FIG. 1: The decay branching ratios of B' to Wt, bg, bZ and bH, as a function of the B' mass. The couplings are given in the text.

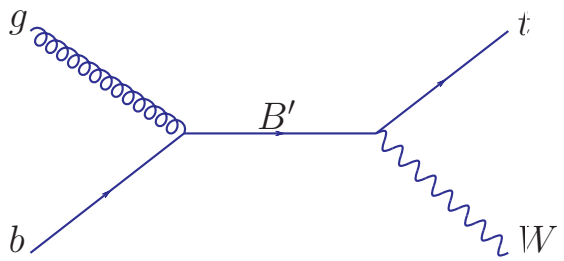

FIG. 2: Feynman diagrams for production of a fourth generation B' quark and decay to a top quark and W boson.

IV. B' PRODUCTION AND DECAY TO tW

We consider the production of B' quarks via the following process,

$$p + p \to B' \to t + W. \tag{8}$$

The Feynman diagram for resonance B' production and decay to Wt is shown in Fig. 2. This process relies on b quark and gluon initial partons. The gluon parton helps the cross section tremendously; however, this process is suppressed by a dimension five anomalous magnetic moment operator (see equation 3) and the b quark initial partons. Notably, the B' quark has access to the full center-of-mass energy of the colliding partons. This increases the ability to probe heavy B' quarks in contrast to B' quark pair production.

In this section we explore the $t\,W$ final state. We also present the production cross section for different B' masses at the LHC for three different beam energies. The total cross section for B' production and subsequent decay to a top quark and W boson at the LHC are computed with Madgraph [29] for several different c.m. energies and the same couplings as in Sec. III A, and are shown in Fig. 3. We use the CTEQ6L1 set of parton distribution functions (PDF) [30] and set the factorization and renormalization scales to the B' mass. The cross section is computed at leading order in QCD. Next-to-leading order corrections to FCNC single top quark production have also been computed, though they do not include corrections to the heavy quark decay [31, 32]. The cross section peaks at about 300 GeV, where the top quark and W boson are both on shell, and then decreases for higher B' masses. This decrease is due in part to the decrease of the parton luminosity and in part to the decreasing $B'gb$ coupling as the B' mass increases. The increasing parton luminosity is visible also in different slopes for the three curves, more so when comparing 14 TeV to the other two. The uncertainty on the cross section for a B' mass of 700 GeV is 0.3% when varying the top quark mass by 1 GeV and 13% when varying the factorization and renormalization scales up and down by a factor of two.

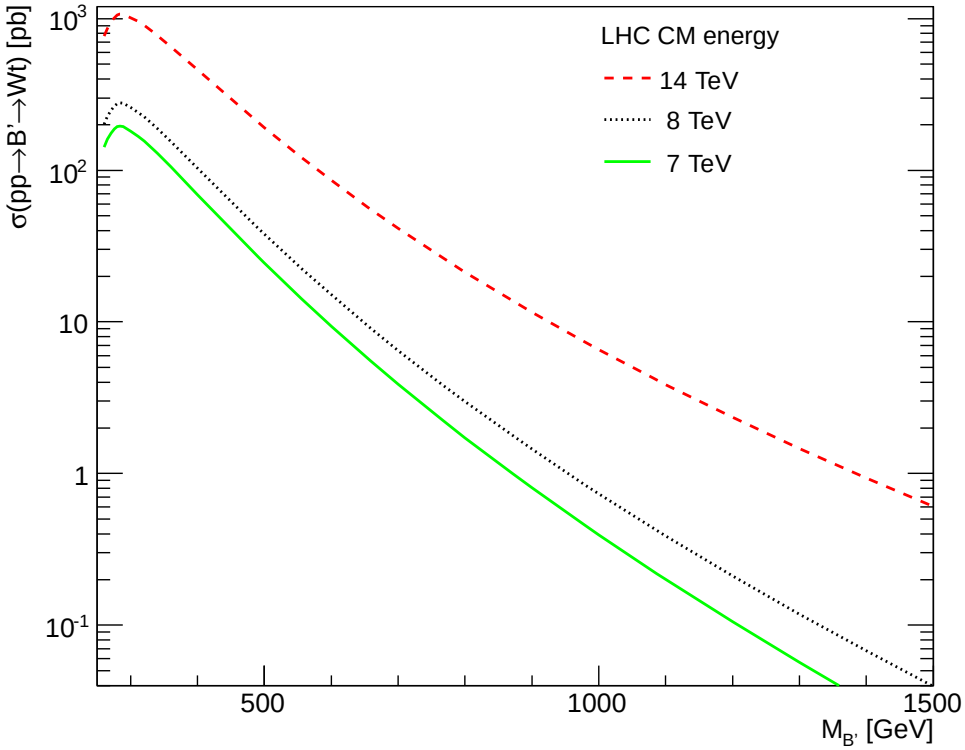

FIG. 3: The total cross section for B' production with decay to tW at the LHC, for $f_L = 1$, $f_R = 0$ and three different c.m. energies.

V. ANALYSIS

The LHC has collected enough events already to look for singly produced B'. Here, an example analysis demonstrates the prospects for observing a B' quark at the 7 TeV LHC. We consider the lepton+jets B' final state and evaluate the backgrounds to this signature. We look at the process $pp \to B \to t\bar{b} \to bl^+\nu\bar{b}$. B' signal events are produced at a benchmark mass of 700 GeV and the numbers of signal and background events remaining after basic selection cuts are computed.

Signal and background events are generated with Madgraph [29] and are normalized to the corresponding LO cross sections. The dominant backgrounds to the final state of lepton and three jets are from top quark pair production and W boson production in association with jets. For top pair production we include both the lepton+jets final state, $t\bar{t} \to bl\nu\,\bar{b}jj$, and the dilepton+jet final state, $t\bar{t}j \to bl\nu\,\bar{b}l\nu\,j$. For the lepton+jets final state, one of the jets must be at low P_T or otherwise be lost in order to enter the signal region. For the dilepton+jet final state, one of the leptons must be at low P_T or otherwise be lost. Smaller backgrounds are from single top quark production in association with a W boson ($t+W$) or with jets ($t+jets$, t-channel and s-channel) and from diboson+jet (WV) production.

We use the anti-kt algorithm in the FastJet [33] package to cluster quarks and gluons into final state jets with parameter $R = 0.4$. Detector resolution effects are simulated by smearing jet and leptonic energies according to a Gaussian:

$$\frac{\delta E}{E} = \frac{\mathcal{A}}{\sqrt{E/\mathrm{GeV}}} \oplus \mathcal{B}\,, \tag{9}$$

where $\frac{\delta E}{E}$ is the energy resolution, $\mathcal{A}$ is a sampling term, $\mathcal{B}$ is a constant term, $\oplus$ represents addition in quadrature, and all energies are measured in GeV. For leptons we take $\mathcal{A} = 5\%$ and $\mathcal{B} = 0.55\%$, while for jets we take $\mathcal{A} = 100\%$ and $\mathcal{B} = 5\%$, chosen to represent the ATLAS and CMS detector performance [34, 35]. We do not smear $\not\!\!E_T$. We model b-tagging as a flat 60% probability to tag b-quark jets and a 0.5% probability to mistag non-b-quark jets (including charm quarks).

Signal and background events are required to pass the following basic selection cuts:

$$\begin{aligned}
\text{At least two jets with} \quad & p_T^j \geq 25\,\text{GeV}, \quad |\eta_j| \leq 2.5 \\
\text{Exactly one lepton with} \quad & p_T^\ell \geq 25\,\text{GeV}, \quad |\eta_\ell| \leq 2.5, \\
\text{Missing energy} \quad & \not\!\!E_T > 25\ \text{GeV}, \\
\text{Object separation} \quad & \Delta R_{jj,j\ell} > 0.4, \quad \Delta R_{\ell\ell} > 0.2.
\end{aligned} \tag{10}$$

The kinematic distribution of the B' signal and the various backgrounds after these cuts are shown in Fig. 4. The backgrounds are mostly at low P_T, whereas the B' signal is at high P_T. The top quark pair background extends farthest into the B' signal region. This can also be clearly seen in the distribution of H_T, the scalar sum of the P_T of all final state objects.

To isolate the B' signal and suppress the SM backgrounds, a set of final cuts is applied on the jet P_T and on H_T,

$$\begin{aligned}
p_T^{\text{jet 1}} &\geq 80\,\text{GeV}, \\
p_T^{\text{jet 2}} &\geq 50\,\text{GeV}, \\
p_T^{\text{jet 3}} &\geq 40\,\text{GeV}, \\
H_T &\geq 425\,\text{GeV}.
\end{aligned} \tag{11}$$

To suppress the background from W+jets and dibosons further, we require at least one jet to be b-tagged.

These cuts effectively suppress most of the SM backgrounds while passing much of the B' signal. The distribution of H_T after the final cuts is shown in Fig. 5. The largest remaining background contribution is from top pair production. At low H_T, W+jets also contributes, less so at high H_T.

The final set of cuts effectively isolates a B' signal at any mass above 600 GeV. In order to further improve the sensitivity of the analysis, the reconstruction of the B' quark and its invariant mass is required. For this reconstruction it is necessary to first obtain the neutrino momentum. We assign $\not\!\!E_T$ to the transverse components of the neutrino momentum and compute the longitudinal component from a W boson mass constraint [36]. The longitudinal momentum of the neutrino $p_{\nu L}$ is formally expressed as

$$p_{\nu L} = \frac{1}{2\,p_{eT}^2}\left(A\,p_{eL} \pm E_e\sqrt{A^2 - 4\,p_{eT}^2\not\!\!E_T^2}\right), \tag{12}$$

where $A = M_W^2 + 2\,\vec{p}_{eT}\cdot\vec{\not\!\!E}_T$. If $A^2 - 4\,p_{eT}^2\not\!\!E_T^2 > 0$, then there are two solutions and we pick the one with smaller $|p_{\nu L}|$. Otherwise the square root is complex and we pick the real part only.

With the neutrino identified properly, we reconstruct the mass of the B' quark as

$$m_{B'}^{\text{rec}} = m(\vec{p}_\nu + \vec{p}_l + \vec{p}_{\text{jet 1}} + \vec{p}_{\text{jet 2}} + \vec{p}_{\text{jet 3}}) \tag{13}$$

We then impose a window cut on the invariant mass difference between the reconstructed invariant mass and the theory B' mass under consideration,

$$\left|m_{B'}^{\text{rec}} - m_{B'}^{\text{theory}}\right| < 100\ \text{GeV}\,. \tag{14}$$

Table I shows the number of events passing each set of cuts, in units of fb.

About half of the signal events pass the basic selection cuts. Only a third of the signal events pass the final selection cuts including b-tagging, but the background is reduced by a factor of 342. In particular the b-tagging cut reduces the W+jets background significantly. The mass window cut leaves a signal:background of 1:2 with sufficient events remaining to be able to discover or rule out a B' at this mass. Even for a B' mass of 1 TeV there are still 12 fb events remaining after the mass window cut, with a background that is reduced

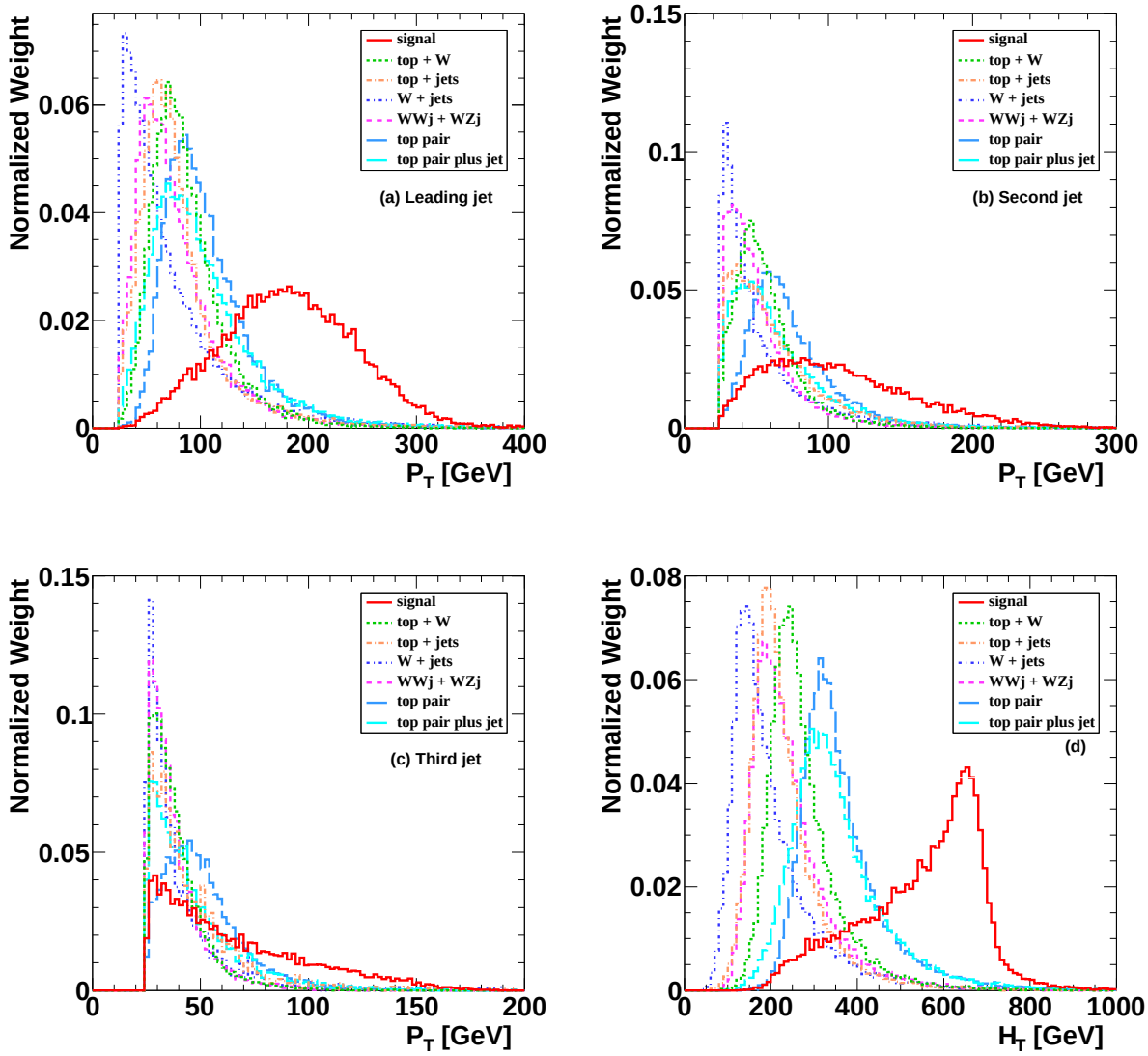

FIG. 4: The distribution of (a) P_T of the leading jet, (b) P_T of the second jet, (c) P_T of the third jet and (d) H_T of all final state objects for the B' signal and backgrounds after basic selection cuts. Each distribution is normalized to unit area.

by a factor of two, hence LHC searches should be sensitive to this mass range with the data already recorded in 2011.

Figure 6 shows the reconstructed invariant mass. The signal peak is clearly visible above the smoothly falling background.

If a B' is found, then it is possible to determine if it has left-handed or right-handed couplings by looking at the W boson helicity from the top quark decay. Figure 7 shows the $cos\theta_{lt}$ distribution, where θ_{lt} is the angle between the lepton in the top quark rest frame and the top quark moving direction in the c.m. frame. At the parton (truth) level before any selection cuts, this results in the familiar SM-like distribution for left-handed B'. The right-handed B' distribution is quite different, and the clear distinction remains even after selection cuts.

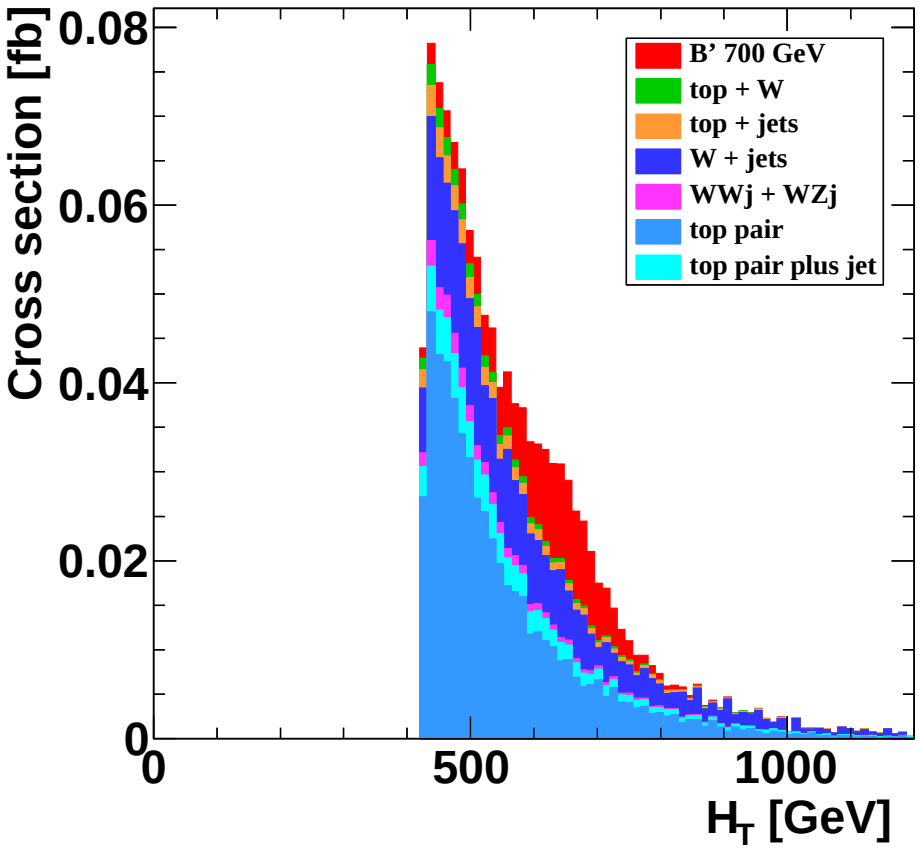

FIG. 5: H_T distribution for the B' signal and backgrounds normalized to their production cross sections after the final cuts.

TABLE I: Cross sections for signal background processes at the 7 TeV LHC passing selection cuts.

σ [fb]	Signal	$t+$jets	$t+W$	$t\bar{t}$	$t\bar{t}j$	WV	$W+$jets	total Bkg.
no cuts	1062	18,877	2,861	22,200	7,900	10,007	2,457,400	2,519,245
basic cuts	507	4,035	808	5,491	772	1,692	92,521	105,319
+ jet p_T cuts	346	282	163	3,117	297	324	27,645	31,828
+ H_T cuts	295	100	46	1,163	205	132	13,120	14,766
+ b-tagging	177	48	27	552	90	34	294	1,045
+ mass window	156	18	10	151	30	12	87	308

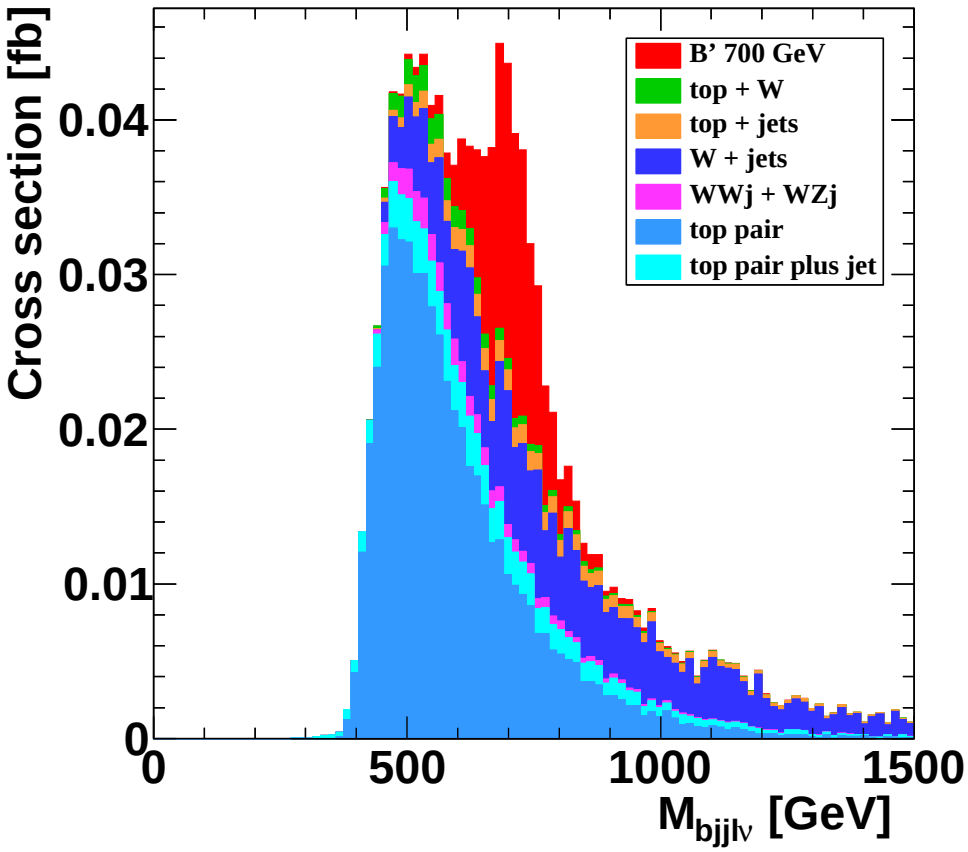

FIG. 6: Reconstructed invariant mass for signal and backgrounds in the B' analysis. The signal and backgrounds are normalized to their production cross sections.

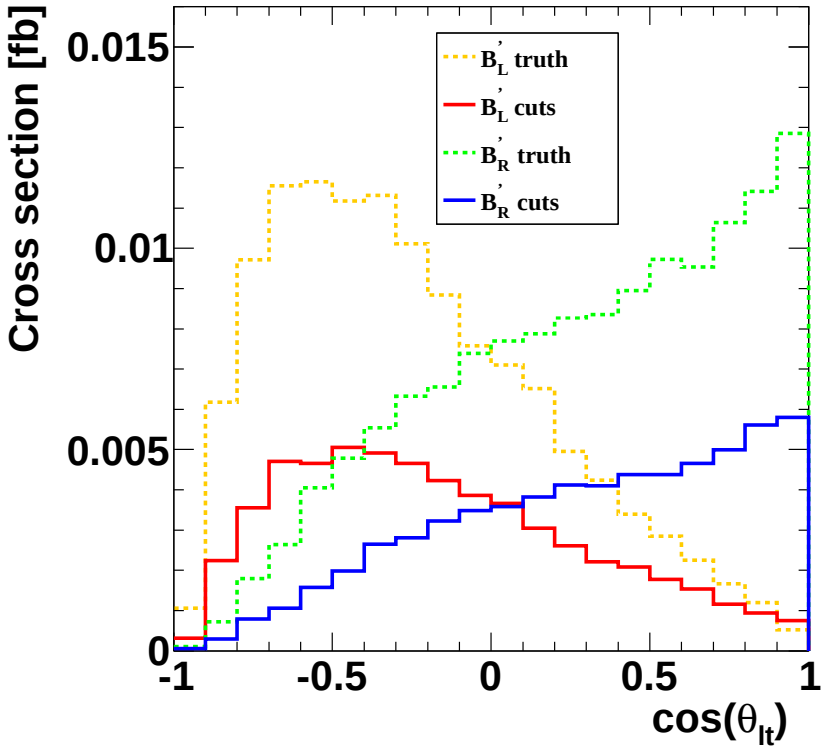

FIG. 7: Angular correlation $\cos\theta$ between the final state lepton and the top moving direction for two different B' models.

VI. CONCLUSIONS

We have presented a model for fourth generation B' quarks and their single production at the LHC with an effective Lagrangian that results in a $B'gb$ coupling. We have presented the B' decay branching ratios and production cross section at the LHC at several c.m. energies. A phenomenological analysis shows that the LHC is sensitive to B' quark production and decay to a single top quark and W boson. The experimental reach should be better than 700 GeV already at the 7 TeV LHC, which makes this a very promising search channel. Moreover, once a B' quark is found, spin correlation in the Wt final state can be used to determine whether it is left-handed or right-handed.

Acknowledgments

The work of J.N. and R.S. was supported in part by the U.S. National Science Foundation under Grant No. PHY-0952729. D.W. is supported in part by a grant from the US National Science Foundation, grant NSF-PHY-0705682, the LHC Theory Initiative. The work of J.H.Y. was supported in part by the U.S. National Science Foundation under Grant No. PHY-0855561.

Appendix

A. Generalized B' Couplings with the SM and the Associated Branching Fractions

Assuming the electroweak anomalous magnetic moment is suppressed compared to the colored anomalous magnetic moment, the Lagrangian for the electroweak couplings of the B' quark is

$$\begin{aligned}\mathcal{L} &= \frac{g_2}{\sqrt{2}} W^-_\mu \bar{t}\gamma^\mu (f_L P_L + f_R P_R) B' + \frac{g_2}{2c_W} Z_\mu \bar{b}\gamma^\mu (F_L P_L + F_R P_R) B' \\ &+ \frac{m_b}{v} h\, \bar{b}\, (y_L P_L + y_R P_R) B' + h.c.\,, \end{aligned} \tag{15}$$

where $\frac{m_b}{v} = \frac{g_2}{2}\frac{m_b}{m_W}$. As a reminder, g_2 is the $SU(2)_L$ coupling and m_b is the bottom quark mass. Here $f_{L,R}$, $F_{L,R}$ and $y_{L,R}$ parametrizes the chirality of the B' coupling with the different SM bosons. $P_{L,R}$ are the traditional projection operators. It is straightforward to compute the partial decay widths of the B' quark as

$$\Gamma(B' \to b\, Z) = \frac{g_2^2}{128\pi c_W^2} \frac{M_{B'}^3}{M_Z^2} (F_L^2 + F_R^2)(1 - x_Z^2)^2 (1 + 2x_Z^2),, \tag{16}$$

$$\Gamma(B' \to t\, W^-) = \frac{g_2^2}{64\pi} \frac{M_{B'}^3}{M_W^2} (f_L^2 + f_R^2)(1 - x_t^2)^3 + \mathcal{O}(x_W^2)\,, \tag{17}$$

$$\Gamma(B' \to b\, h) = \frac{g^2}{128\pi} \frac{M_{B'}^3}{M_W^2} (y_L^2 + y_R^2)(1 - x_h^2)^2\,, \tag{18}$$

$$\Gamma(B' \to b\, g) = \frac{g_s^2}{12\pi} M_{B'} (\kappa_L^2 + \kappa_R^2)\,. \tag{19}$$

Here we define $x_Z = M_Z/M_{B'}$, $x_W = M_W/M_{B'}$, $x_h = M_h/M_{B'}$ and $x_t = M_t/M_{B'}$. As a reminder, g_s is the strong coupling constant. Note that the general decay width $F \to f\, h$ is

$$\Gamma(F \to f\, h) = \frac{g^2}{32\pi} M_F \lambda^{1/2}\left(x_h^2, x_f^2\right) \left[(y_L^2 + y_R^2)(1 + x_f^2 - x_h^2) + 4x_f \mathrm{Re}(y_L y_R^*)\right]\,, \tag{20}$$

where λ is given by

$$\lambda\left(x_h^2, x_f^2\right) = 1 + x_h^4 + x_f^4 - 2x_h^2 - 2x_f^2 - 2x_h^2 x_f^2\,. \tag{21}$$

[1] ATLAS Collaboration, Phys. Lett. B **716**, 30 (2012).
[2] CMS Collaboration, Phys. Lett. B **716**, 1 (2012).
[3] S. Weinberg, Phys. Rev. D **13**, 974 (1976); L. Susskind, Phys. Rev. D **20**, 2619 (1979).
[4] C. T. Hill, Phys. Rev. D **24**, 691 (1981); C. T. Hill, Phys. Lett. B **266**, 419 (1991); R. S. Chivukula, B. A. Dobrescu, H. Georgi and C. T. Hill, Phys. Rev. D **59**, 075003 (1999).
[5] B. A. Dobrescu and C. T. Hill, Phys. Rev. Lett. **81**, 2634 (1998).
[6] C. T. Hill and E. H. Simmons, Phys. Rept. **381**, 235 (2003) [Erratum-ibid. **390**, 553 (2004)] and references therein.
[7] D. B. Kaplan, H. Georgi and S. Dimopoulos, Phys. Lett. B **136**, 187 (1984).
[8] N. Arkani-Hamed, A. G. Cohen and H. Georgi, Phys. Lett. B **513**, 232 (2001); N. Arkani-Hamed, A. G. Cohen, E. Katz and A. E. Nelson, JHEP **0207**, 034 (2002).
[9] N. Arkani-Hamed, S. Dimopoulos and G. R. Dvali, Phys. Lett. B **429**, 263 (1998).
[10] L. Randall and R. Sundrum, Phys. Rev. Lett. **83**, 3370 (1999).
[11] CMS Collaboration, Phys. Rev. Lett. **107**, 091802 (2011).
[12] ATLAS Collaboration, arXiv:1205.3130 [hep-ex].
[13] ATLAS Collaboration, arXiv:1205.5764 [hep-ex].
[14] N. Kidonakis, Phys. Rev. D **83**, 091503 (2011); N. Kidonakis, Phys. Rev. D **81**, 054028 (2010); N. Kidonakis, Phys. Rev. D **82**, 054018 (2010).
[15] ATLAS Collaboration, arXiv:1202.6540 [hep-ex].
[16] CMS Collaboration, JHEP **1205**, 123 (2012).
[17] CDF Collaboration, Phys. Rev. Lett. **106**, 141803 (2011).
[18] D0 Collaboration, Phys. Rev. Lett. **106**, 081801 (2011).
[19] ATLAS Collaboration, [arXiv:1204.1265 [hep-ex]].
[20] ATLAS Collaboration, Phys. Lett. B **712**, 22 (2012).
[21] M. S. Chanowitz, M. A. Furman and I. Hinchliffe, Phys. Lett. B **78**, 285 (1978).
[22] M. S. Chanowitz, M. A. Furman and I. Hinchliffe, Nucl. Phys. B **153**, 402 (1979).
[23] M. E. Peskin and T. Takeuchi, Phys. Rev. D **46**, 381 (1992).
[24] K. Nakamura *et al.* [Particle Data Group Collaboration], J. Phys. G G **37**, 075021 (2010).
[25] K. Agashe, R. Contino, L. Da Rold and A. Pomarol, Phys. Lett. B **641**, 62 (2006).
[26] R. Sekhar Chivukula, S. Di Chiara, R. Foadi and E. H. Simmons, Phys. Rev. D **80** (2009) 095001 [Erratum-ibid. D **81** (2010) 059902].
[27] A. Kagan, In *Santa Barbara 1997, Heavy flavor physics* 215-243 [hep-ph/9806266].
[28] U. Baur, I. Hinchliffe and D. Zeppenfeld, Int. J. Mod. Phys. A **2**, 1285 (1987).
[29] J. Alwall, M. Herquet, F. Maltoni, O. Mattelaer and T. Stelzer, JHEP **1106**, 128 (2011). We use MadGraph 5 version 1.3.
[30] J. Pumplin, D. R. Stump, J. Huston, H. L. Lai, P. M. Nadolsky and W. K. Tung, JHEP **0207**, 012 (2002).
[31] J. Gao, C. S. Li, J. J. Zhang and H. X. Zhu, Phys. Rev. D **80**, 114017 (2009).
[32] J. A. Aguilar-Saavedra, Nucl. Phys. B **837**, 122 (2010).
[33] M. Cacciari, G. P. Salam and G. Soyez, Eur. Phys. J. C **72**, 1896 (2012).
[34] ATLAS Collaboration, JINST **3**, S08003 (2008).
[35] CMS Collaboration, J. Phys. G G **34**, 995 (2007).
[36] G. L. Kane and C. P. Yuan, Phys. Rev. D **40**, 2231 (1989).
[37] In the limit of exact custodial symmetry, the mass of the top and bottom partners are the same. Thus, the T parameter goes to zero.
[38] This scenario is possible if, above the cutoff, new quarks transforming as a N of $SU(2)_L$ with hypercharges $Y = \frac{1}{6}(1-3N)$, $\frac{1}{6}(1-3(N-2))$, $\frac{1}{6}(1-3(N-4)), \ldots$, are added in various anomaly free combinations. Here the number of different hypercharges is the dimension of N. After (all of) the symmetry breaking, the fermions with $Q = -1/3$ mixes with the SM bottom quark.